A double radio halo in the close pair of galaxy clusters Abell 399 and Abell 401

M. Murgia[1,2], F. Govoni[1], L. Feretti[2], and G. Giovannini[2,3]

[1] INAF - Osservatorio Astronomico di Cagliari, Poggio dei Pini, Strada 54, 09012 Capoterra (CA), Italy
   e-mail: m.murgia@ira.inaf.it
[2] INAF - Istituto di Radioastronomia, via Gobetti 101, 40129 Bologna, Italy
[3] Dipartimento di Astronomia, Univ. Bologna, via Ranzani 1, 40127 Bologna, Italy

ABSTRACT

Aims. Radio halos are faint radio sources usually located at the center of merging clusters of galaxies. These diffuse radio sources are rare, having so far been found only in about 30 clusters of galaxies, suggesting that particular conditions are needed to form and maintain them. It is interesting to investigate the presence of radio halos in close pairs of interacting clusters in order to possibly clarify their origin in relation to the evolutionary state of the merger. In this work, we study the case of the close pair of galaxy clusters A399 and A401.
Methods. A401 is already known to contain a faint radio halo, while a hint of diffuse emission in A399 has been suggested based on the NVSS. To confirm this possibility, we analyzed deeper Very Large Array observations at 1.4 GHz of this cluster.
Results. We find that the central region of A399 is permeated by a diffuse low-surface brightness radio emission that we classify as a radio halo with a linear size of about 570 kpc and a central brightness of 0.3 μJy/arcsec^2. Indeed, given their comparatively small projected distance of ∼3 Mpc, the pair of galaxy clusters A401 and A399 can be considered as the first example of double radio halo system. The discovery of this double halo is extraordinary given the rarity of these radio sources in general and given that current X-ray data seem to suggest that the two clusters are still in a pre-merger state. Therefore, the origin of the double radio halo is likely to be attributed to the individual merging histories of each cluster separately, rather than to the result of a close encounter between the two systems.

Key words. galaxies: clusters: individual: Abell 399 – radio continuum: galaxies – galaxies: clusters: individual: Abel 401

1. Introduction

An ever increasing number of galaxy clusters exhibit Mpc-scale synchrotron radio halos associated with the intracluster medium. These elusive radio sources are located at the cluster center and are characterized by a regular shape and extremely low surface brightness at levels of ∼1 μJy/arcsec^2 at 1.4 GHz. To date, about 30 radio halos are known (see Giovannini et al. 2009, for recent compilation), and most have been found in clusters that show significant evidence of an ongoing merger (e.g. Buote 2001). The rarity of radio halos seems to suggest that particular conditions are required for their formation and maintenance. Merger events may play a strong role in the re-acceleration of the radio-emitting relativistic particles, thus providing the energy that powers these extended sources (e.g. Brunetti et al. 2009). In this context, it is interesting to investigate radio halos in close pairs of interacting clusters of galaxies. These systems may share the same recent dynamical history, so they are unique laboratories for studying the formation of radio halos and possibly clarifying the origin of these radio sources in relation to the evolutionary state of the merger.

In this work we analyze the close pair of galaxy clusters A399 and A401, which are located at a redshift of z = 0.071806 and z = 0.073664 (Oegerle & Hill 2001). This is an exceptional pair, since the two clusters are separated in projection by an angular distance of 36′, corresponding to a linear separation of 3 Mpc in our chosen cosmology (see below). A399 and A401 are two rich clusters of galaxies with a similar average gas temperature of $kT \simeq 7$ and $kT \simeq 8$ keV, respectively. The

X-ray luminosities in the 0.1−2.4 keV band for the two clusters are L_X = 3.8 and 6.5×10^{44} erg/s (Reiprich & Böhringer 2002). The X-ray excess and the slight temperature increase in the region between the two clusters indicate a physical link between this pair of clusters (e.g. Fujita et al. 1996; Fabian et al. 1997; Markevitch et al. 1998). Recent XMM X-ray analyses (Sakelliou & Ponman 2004; Bourdin & Mazzotta 2008) show that neither of the two clusters contains a cooling core. However, the reasonably relaxed morphology of the clusters and the absence of major temperature anomalies argue against models in which A399 and A401 have already experienced a close encounter. The link region between A399 and A401 has been studied with the Suzaku satellite by Fujita et al. (2008). The metallicity of the hot intergalactic medium in this region is found to be comparable to those in the inner regions of the clusters. The authors conclude that the metal enrichment in this region is likely caused by strong winds from galaxies before the cluster formation rather than by cluster collision. These analyses indicate that the clusters are just starting to mildly interact and that the sub-features found in their inner regions are related to the individual merging histories of each cluster separately, rather than to the remnant of a previous merger of the two systems. Indeed, in the light of all these indications, it seems likely that A399 and A401 are two merger remnants, just before they merge together to form a single rich cluster of galaxies.

A401 is already known to contain a faint radio halo (Harris et al. 1980; Roland et al. 1981; Giovannini et al. 1999; Bacchi et al. 2003), while a hint for a diffuse emission in A399 has
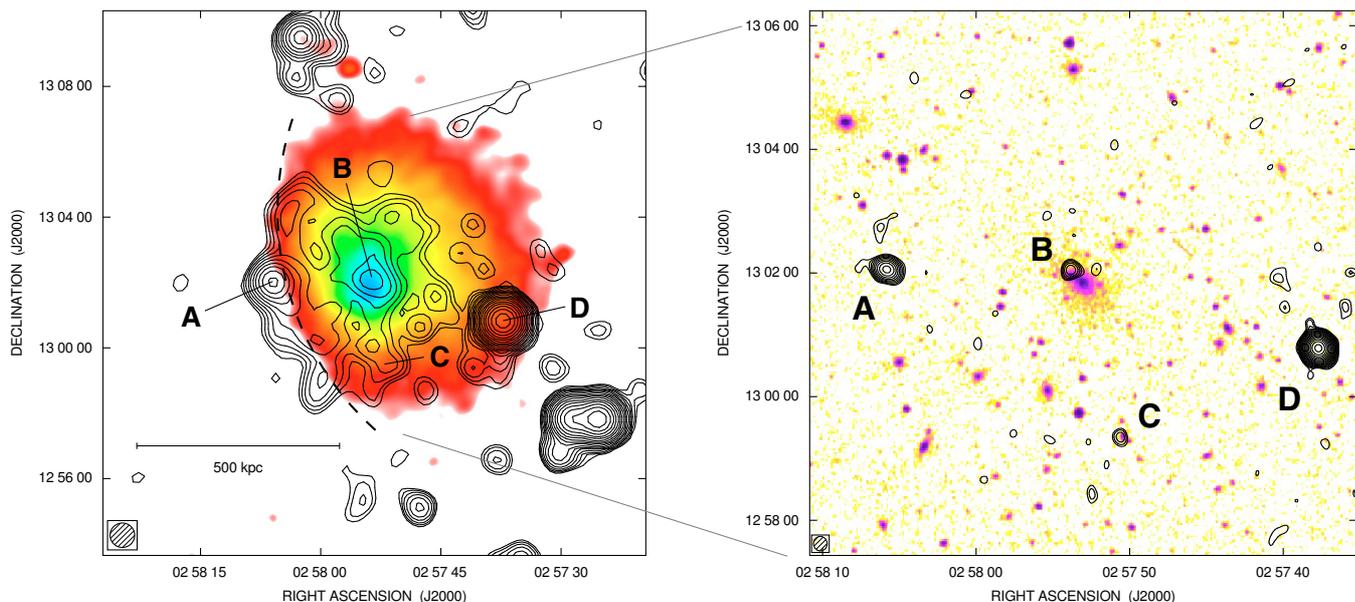
Fig. 1. *Left*: total intensity radio contours of A399 at 1.4 GHz with the VLA in D configuration. The image has an *FWHM* of $45'' \times 45''$. The first contour level is drawn at 120 μJy/beam and the rest are spaced by a factor of $\sqrt{2}$. The sensitivity (1σ) is 40 μJy/beam. The total intensity radio contours overlaid on the XMM X-ray image in the 0.2–12 keV band. The X-ray image has been convolved with a Gaussian of $\sigma = 12''$. *Right*: zoom of the total intensity radio contours in the center of A399 at 1.4 GHz with the VLA in C array. The image has an *FWHM* of $14'' \times 13''$. The first contour level is drawn at 120 μJy/beam and the others are spaced by a factor of $\sqrt{2}$. The sensitivity (1σ) is 40 μJy/beam. The contours of the radio intensity are overlaid on the optical DSS2 image.

been suggested by Sakelliou & Ponman (2004) based on the NRAO VLA Sky Survey (NVSS) images. In this letter, we report on the results of deeper observations performed at 1.4 GHz with Very Large Array (VLA) in C and D configurations.

Throughout this paper we assume a ΛCDM cosmology with $H_0 = 71$ km s^{-1} Mpc^{-1}, $\Omega_{\rm m} = 0.27$, and $\Omega_{\Lambda} = 0.73$. At the distance of A399, $1''$ corresponds to 1.35 kpc.

2. Radio observations of A399

The cluster of galaxies A399 was observed with the VLA at 1.4 GHz in the C and D configurations on April and August 2004, respectively (program AS791). The two observations have the same pointing, RA = 02$^{\rm h}$57$^{\rm m}$54$^{\rm s}$ and Dec = +13°01$'$34$''$(J2000). They also share the same observing IF frequencies, 1415/1465 MHz, and bandwidth, 50 MHz. The total time on source is of 2.2 and 1.5 h in C and D configurations, respectively.

Calibration and imaging were performed with the NRAO Astronomical Image Processing System (AIPS). The data were calibrated in both phase and amplitude. The phase calibration was completed by using the nearby secondary calibrator 0321+123 observed at intervals of ~30 min. The flux-density scale was calibrated by observing 0137+331 (3C 48). Total intensity images were produced following the standard procedures: Fourier-Transform, Clean, and Restore. Several cycles of self-calibration were applied in order to remove residual phase variations.

From the D configuration data, we produced an image with a circular *FWHM* beam of $45'' \times 45''$ and a noise of 40 μJy/beam (1σ level). The C configuration data resulted in an image with an *FWHM* beam of $14'' \times 13''$ and a noise level of 40 μJy/beam.

3. Results

3.1. A new radio halo in A399

We present the new radio image of A399, taken with the VLA in D configuration at 1.4 GHz, in the left panel of Fig. 1. The radio iso-contours are overlaid on the MOS1+MOS2 XMM-Newton image of the cluster X-ray emission in the 0.2–12 keV band (Obs. id: 0112260101). The relatively large beam of the radio observation provides an optimal S/N ratio to the low-surface brightness emission. We find that the central region of A399 is permeated by a very low-surface brightness diffuse emission which is classified as a radio halo. The halo has an angular size, as measured from the 3σ radio isophote, of about 420$''$. The corresponding linear size is $LLS \simeq 570$ kpc. The radio halo is significantly smaller than the maximum angular size visible by the VLA D array at this frequency, i.e. 900$''$. This ensures that we should have recovered most of the flux density from the extended radio emission. The morphology of the halo is quite regular, although an arc-like feature (indicated by a dashed curved line in Fig. 1) of enhanced radio emission is observed in correspondence of the sharp X-ray edge to the east of the cluster core reported by Sakelliou & Ponman (2004) and Bourdin & Mazzotta (2008). The X-ray surface brightness left to the edge cut offs sharply and, as a consequence, the overall X-ray cluster morphology appears to be elongated to the north-west. Sakelliou & Ponman (2004), based on the results of the numerical simulations from Takizawa (1999), attributed the origin of the X-ray edge to the infall of a low mass system travelling east to west into A399. The radio feature could be originated by a relatively faint shock in the intracluster medium due to the merging of this low mass system.

We used the higher resolution of the C configuration image to separate the diffuse cluster emission from that of the unrelated discrete radio sources. A zoom of the inner $8' \times 8'$ region of A399 is shown in the right panel of Fig. 1. The total intensity
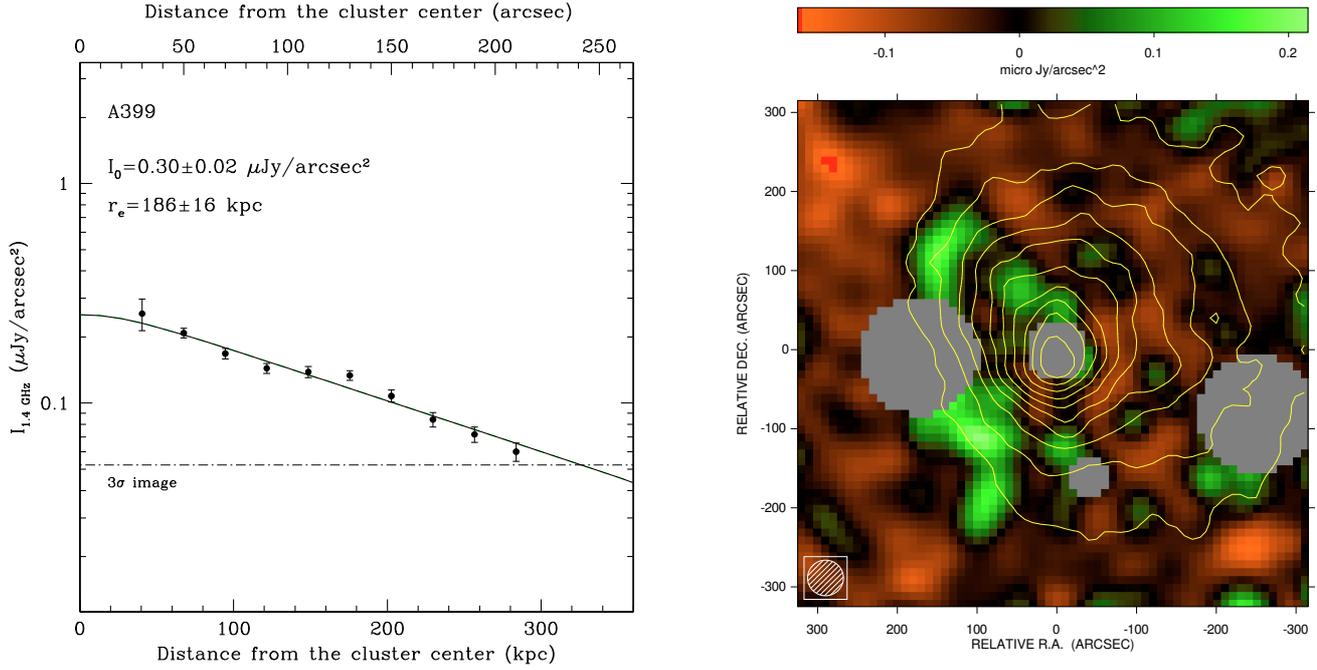
Fig. 2. *Left*: the azimuthally averaged brightness profile of the radio halo emission in A399. The profile is calculated in concentric annuli and all the discrete sources have been masked. The horizontal dashed-dotted line indicates the 3σ noise level of the radio image while the continuous line indicates the best fit profile described by an exponential law (see text). *Right*: overlay of the XMM X-ray contours on the fit residuals, gray regions correspond to the masked discrete radio sources.

radio contours of the VLA observation in C array are overlaid on the DSS2 red plate image[1] of the cluster. The C configuration image indicates clearly that the radio halo is not due to the blending of discrete sources. In fact, we can identify just four discrete radio sources seen in projection over the halo. The source on the left of the halo (labeled A in Fig. 1) has a flux density of $S_{1.4} \simeq 2.5 \pm 0.07$ mJy. There is no optical counterpart for radio source A in the DSS2 image. A second faint source (labeled B; $S_{1.4} \simeq 0.7 \pm 0.04$ mJy) is visible near the cluster center. The overlay with the optical image shows that this discrete radio source is associated to a faint galaxy located $14''$ to the north-east of the cD galaxy which, on the contrary, appears to be radio quite. The small galaxy associated with radio source B has a redshift of $z = 0.07691$ (Hill & Oegerle 1993), and therefore it is likely a member of A399. A third very faint source (labeled C; $S_{1.4} \simeq 0.3 \pm 0.04$ mJy) is located in the south region of the halo. Source C has a clear optical counterpart in the DSS2 image but no redshift information is available in the literature. Finally, the stronger discrete source (labeled D) is located on the extreme right side of the radio halo and has a flux density of $S_{1.4} \simeq 36.8 \pm 1.1$ mJy. There is no optical counterpart for radio source D in the DSS2 image.

In the left panel of Fig. 2 we show the azimuthally averaged radio halo brightness profile obtained from the D configuration image at $45''$ resolution after the correction for the primary beam attenuation. Each data point represents the average brightness in concentric annuli of half beam width. Discrete sources have been masked out and excluded from the statistics. The observed brightness profile is traced down to a level of 3σ. Following Murgia et al. (2009), we modeled the radio halo brightness profile, $I(r)$, with an exponential of the form $I(r) = I_0 e^{-r/r_e}$, whose best fit is represented by the solid line in Fig. 2. The fit is performed in the image plane as described in Murgia et al. (2009).

In order to properly take into account the resolution, the exponential model is first calculated in a 2-dimensional image, with the same pixel size and field of view as that observed, and then convolved with the same beam by means of a Fast Fourier Transform. The resulting image is masked exactly in the same regions as for the observations. Finally, the model is azimuthally averaged with the same set of annuli used to obtain the observed radial profile. All these functions are performed at each step during the fit procedure. As a result, the values of the central brightness, I_0, and the e-folding radius r_e provided by the fit are deconvolved quantities and their estimate includes all the uncertainties related to the masked regions and to the sampling of the radial profile in annuli of finite width. The best fit of the exponential model yields a central brightness of $I_0 = 0.3 \pm 0.02$ μJy/arcsec^2 and $r_e = 186 \pm 16$ kpc with a reduced $\chi^2 = 1.6$. The halo flux density obtained by integrating the radio brightness profile up to the 3σ isophote and excluding the discrete sources is of $S_{1.4} = 16.0 \pm 2$ mJy, which corresponds to a radio power of $P_{1.4} \simeq 2 \times 10^{23}$ W/Hz. In the right panel of Fig. 2, we show the overlay of the XMM X-ray contours on the residuals obtained by subtracting the best fit from the observed radio halo image. The most striking feature emerging in the residuals is the arc-like structure mentioned above. The radio arc appears to be co-incident, at least in projection, with the sharp edge of the X-ray cluster emission.

In Fig. 3, we show the best fit central brightness I_0 versus the length-scale r_e of A399 in comparison with the set of radio halos analyzed in Murgia et al. (2009). A399 is somewhat fainter than A401 but twice as large. These characteristics made it the cluster with the lowest synchrotron emissivity $J_{1.4} = 1.6 \times 10^{-43}$ erg s^{-1} cm^{-3} Hz^{-1}. Despite its low emissivity, the physical properties of the small radio halo in A399 are in good agreement with the extrapolation of the properties of the giant ($LLS > 1$ Mpc) radio halos presented in Giovannini et al. (2009). In particular, the correlation between the LLS and the

---

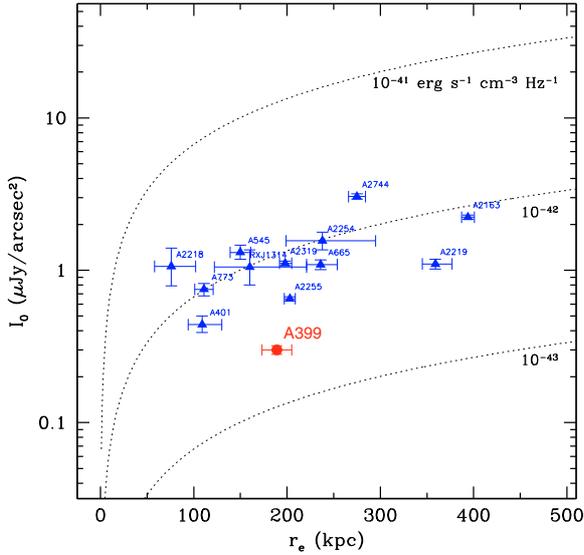[1] See http://archive.eso.org/dss/dss

Fig. 3. Best fit central brightness I_0 versus the length-scale r_e of A399 in comparison with the set of radio halos analyzed in Murgia et al. (2009). The dotted lines indicate regions of constant synchrotron emissivity.

radio power and between the X-ray luminosity and radio power are in good agreement, confirming that small size and giant radio halos may have similar origin and properties.

3.2. The double radio halo in the A399–A401 system

By combining the new D configuration image of A399 presented in this work and the radio image of A401 obtained by Bacchi et al. (2003), we produced a wide field image of the A399–A401 complex. The individual images of the two galaxy clusters have been taken with the same VLA configuration and frequency. They are characterized by the same beam, cellsize, and a very similar noise level. Moreover, the two galaxy clusters are located at a projected distance of 36′. Incidentally, this is exactly the size of the primary beam of the VLA antennas at 1.4 GHz. An accurate mosaicing would require the pointings to be spaced by half the primary beam size, however, for illustrative purposes, we combined the two images in a single field that comprises both galaxy clusters through the AIPS task LTESS.

Similarly, we produced a mosaicing of the X-ray emission in the 0.2–12 keV band by combining three different XMM pointings centered on A399 (Obs. id. 0112260101), A401 (Obs. id. 0112260203), and in between the two clusters (Obs. id. 0112260302). We used the tool reproject_image_grid, implemented in the CIAO software (Fruscione et al. 2006), to reproject the MOS1 and MOS2 images of the three pointings to a common frame of reference, creating a mosaic from the individual observations. The final X-ray image has been exposure corrected and smoothed with a Gaussian kernel of $\sigma = 12''$.

In Fig. 4, we present the iso-contours of the radio mosaic overlaid on the mosaic of the X-ray images. The figure clearly shows the diffuse emission in the radio and X-ray bands originating from the intracluster medium of the two clusters. Indeed, we can conclude that the close pair of galaxy clusters A401 and A399 can be considered as the first example of double radio halo system.

The small radio halos in A339 and A401 are among the faintest so far seen in cluster of galaxies (see also Fig. 3). In

A399, the centroid of the radio halo is shifted with respect to the X-ray peak while the halo in A401 has an elongated shape in the same direction of the X-ray emission. Although in a number of clusters a spatial correlation is observed between the radio halo brightness and the X-ray emission (Govoni et al. 2001), the distortions and offsets of the radio emission in A399 and A401 seem to be common properties of small halos. Feretti et al. (2009) analyzed the positions of radio halos with respect to the X-ray gas distribution. Both giant and small radio halos can be significantly shifted, up to hundreds of kpc, with respect to the centroid of the host cluster. Moreover, they found that this effect becomes more relevant when halos of smaller size, like those in A399 and A401, are considered.

4. Discussion

We briefly discuss the discovery of the double radio halo in the A401–A399 system in relation to the evolutionary state of the merger between the two clusters.

4.1. Post-merger scenario

We first consider the scenario in which A399 and A401 are in a post-merger state as early suggested by Fabian et al. (1997). In this case, both radio halos may have formed as a consequence of the dissipation of the energy delivered in a close encounter between the two clusters. In this context, it is interesting to compare the life-time of the synchrotron emitting cosmic ray electrons, t_{syn}, with the time elapsed since the clusters "collision", t_{coll}. The radiative losses due to the inverse Compton scattering of the cosmic microwave background photons limit the age synchrotron electrons radiating at 1.4 GHz to $t_{syn} \lesssim 10^8$ yrs. According to Yuan et al. (2005), the encounter event occurred $t_{coll} \sim 3.5 \times 10^9$ yrs ago and the two clusters are currently separating apart at a true relative velocity of about 580 km s^{-1}. Hence, $t_{coll} \gg t_{syn}$. This implies that the continuing turbulent dissipation of the energy released during the previous encounter between the two clusters should be able to maintain the two radio halos visible long after the collision. However, this amount of time seems to be much longer than the typical time-scale for the dissipation of turbulence in the intracluster medium during cluster mergers, which is ~1 Gyr (Brunetti et al. 2009). Therefore, the post-merger scenario seems not applicable to explain the origin of the double radio halo.

4.2. Pre-merger scenario

The recent X-ray analyses of the A399 and A401 complex by Sakelliou & Ponman (2004) and Bourdin & Mazzotta (2008) disfavour the above scenario and rather indicate that the clusters are just at an early stage of merging and that they are interacting mildly, because their separation is too large for more dramatic effects. In this scenario, the origin of the double radio halo has to be attributed to the individual merging histories of each cluster separately, rather than to the result of a close encounter between the two systems. The two clusters must have experienced a similar sequence of mergers which prevented the formation of the cool cores and left significant residual kinetic energy in the gas to power the radio halos. If the two clusters have formed within a collapsing filament, and are now falling towards one another, then this could increase the probability of the observed association considerably, since they are no longer independent systems.
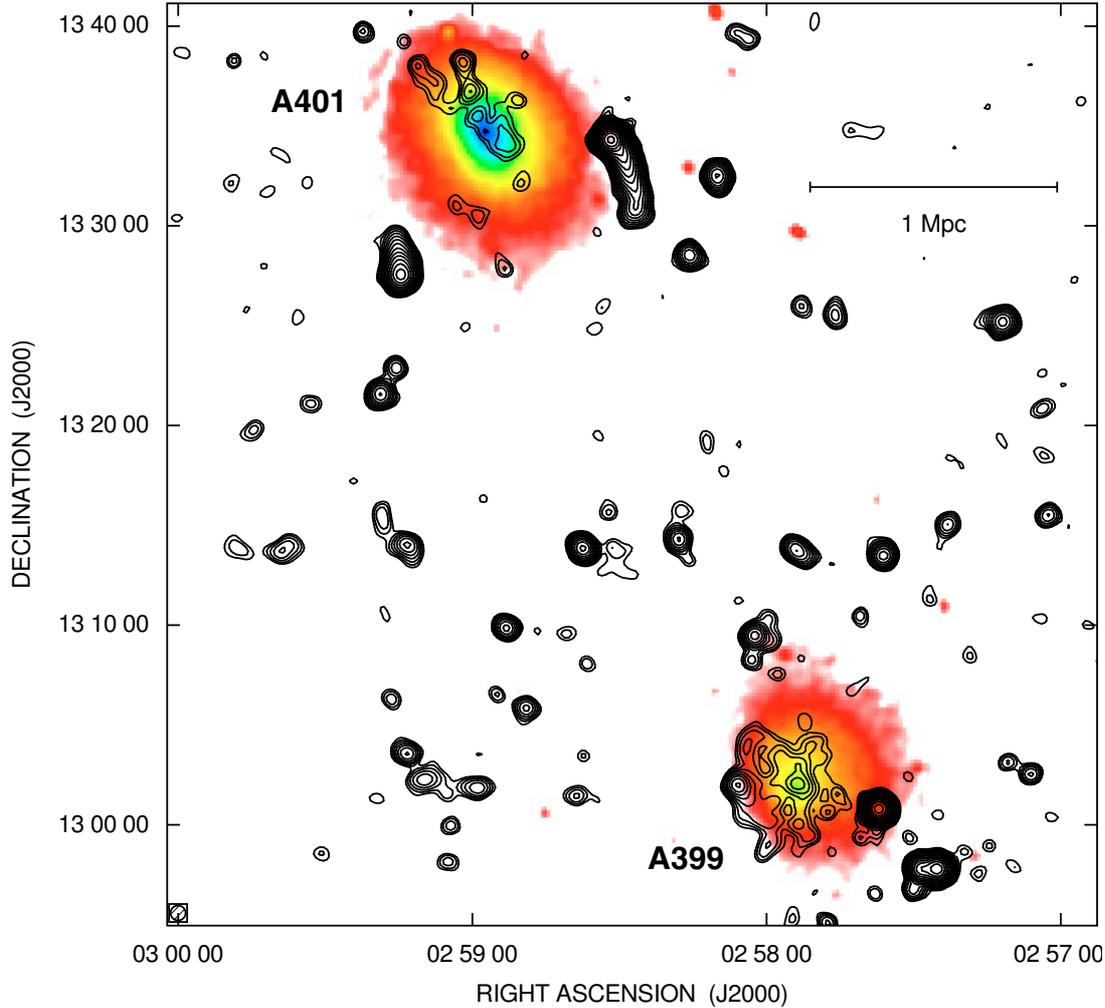
Fig. 4. Total intensity radio contours of the complex A401–A399, obtained by combining the two VLA observations at 1.4 GHz in D configuration of the two clusters, as described in the text. The radio image is shown by the iso-contours and has an *FWHM* of $45'' \times 45''$. The first contour level is drawn at 120 μJy/beam and the rest are spaced by a factor of $\sqrt{2}$. The sensitivity (1σ) is 40 μJy/beam. Total intensity radio contours are overlaid on the XMM X-ray image in the 0.2–12 keV band. The X-ray image has been convolved with a Gaussian kernel of $\sigma = 12''$.

The origin of the double radio halo in A399 and A401 would be indeed a direct consequence of the same environment in which the two clusters formed. This has important implications on the models on the origin of small radio halos since it implies that minor merger play a fundamental role in the formation and maintaining of these diffuse radio sources.

It interesting to note that neither A399 nor A401 are cool core clusters. According to the results of the numerical simulations by Burns et al. (2008), many noncool core clusters undergo major merger early in their history. Smaller mass units with cool cores continue to be accreted by these systems but are usually disrupted by ram pressure within a single core passage. This is what we are probably witnessing in the case of A399. The sharp X-ray edge observed in the X-ray image has been interpreted by Sakelliou & Ponman (2004) as the result of the infall of a smaller sub-unit. In this work we showed that this feature appears to be strictly connected with a bright arc-like structure in the periphery of the radio halo. There are also indirect evidence that A401 is disturbed by a merger since it is elongated, hosts a hot core, and has a complex temperature distribution.

4.3. Tidal interaction

Finally, we may suggest a third scenario in which the formation of the double radio halo is triggered by the long-distance tidal interactions occurring between the two clusters. The presence of non-thermal radio emission could prove that, even if the two sub-clusters are still two distinct entities, their mutual interaction happens to be already experienced by their intracluster media, and would therefore indicate that merger effects can be at work at an early stage of the process. However, the tidal forces should be relevant only in the external regions of the clusters, and not in the central regions occupied by the radio halos, as already noted by Sakelliou & Ponman (2004). Furthermore, it is not clear what mechanism would be able to turn a small tidal acceleration into relativistic particles. Hence, it seems unlikely that the tidal scenario could provide an acceptable explanation for the double radio halo in A401–A399.

5. Conclusions

In summary, we find that the central region of A399 is permeated by a diffuse low-surface brightness radio emission which is

classified as a radio halo with a length-scale of about 190 kpc and a central brightness of 0.3 μJy/arcsec^2. Indeed, given their projected distance of ∼3 Mpc, the pair of galaxy clusters A401 and A399 can be considered as the first example of double radio halo system.

The origin of the double radio halo is likely attributed to the individual merging histories of each cluster separately, rather than to the result of a close encounter between the two systems. The two clusters must have experienced a similar sequence of mergers which prevented the formation of the cool cores and left significant residual kinetic energy in the gas to power the radio halos.

It seems likely that the two small radio halos in A399 and A401 are in proximity to merge together eventually forming a single giant radio halo or a large scale diffuse emission identified with a filamentary supercluster-like structure. This offers new clues to how giant radio halos could form, since it is now clear that magnetic fields and relativistic particles can already be present in the intracluster medium of two clusters well *before* a major merger event between them.

References

Bacchi, M., Feretti, L., Giovannini, G., et al. 2003, A&A, 400, 465
Bourdin, H., & Mazzotta, P. 2008, A&A, 479, 307
Brunetti, G., Cassano, R., Dolag, K., et al. 2009, A&A, 507, 661
Buote, D. A. 2001, ApJ, 553, L15
Burns, J. O., Hallman, E. J., Gantner, B., et al. 2008, ApJ, 675, 1125
Fabian, A. C., Peres, C. B., & White, D. A. 1997, MNRAS, 285, L35
Feretti, L., Bonafede, A., Giovannini, G., Govoni, F., & Murgia, M. 2009 [arXiv:0910.1519]
Fujita, Y., Koyama, K., Tsuru, T., et al. 1996, PASJ, 48, 191
Fujita, Y., Tawa, N., Hayashida, K., et al. 2008, PASJ, 60, 343
Fruscione, A., McDowell, J. C., Allen, G. E., et al. 2006, Proc. SPIE, 6270
Giovannini, G., Tordi, M., & Feretti, L. 1999, New Astron., 4, 141
Giovannini, G., Bonafede, A., Feretti, L., et al. 2009, A&A, 507, 1257
Govoni, F., Enßlin, T. A., Feretti, L., et al. 2001, A&A, 369, 441
Harris, D. E., Kapahi, V. K., & Ekers, R. D. 1980, A&AS, 39, 215
Markevitch, M., Forman, W. R., Sarazin, C. L., et al. 1998, ApJ, 503, 77
Murgia, M., Govoni, F., Markevitch, M., et al. 2009, A&A, 499, 679
Oegerle, W. R., & Hill, J. M. 2001, AJ, 122, 2858
Reiprich, T. H., & Böhringer, H. 2002, ApJ, 567, 716
Roland, J., Sol, H., Pauliny-Toth, I., et al. 1981, A&A, 100, 7
Sakelliou, I., & Ponman, T. J. 2004, MNRAS, 351, 1439
Takizawa, M. 1999, ApJ, 520, 514
Yuan, Q.-R., Yan, P.-F., Yang, Y.-B., et al. 2005, Chin. J. Astron. Astrophys., 5, 126